

Aerodynamic Analysis of Intermodal Freight Trains Using Machine Vision

9th World Congress on Railway Research, May 22-26, 2011

Avinash Kumar

avinash@uiuc.edu

University of Illinois at
Urbana-Champaign
Department of Electrical
and Computer
Engineering
Beckman Institute for
Advanced Science and
Technology
Computer Vision and
Robotics Laboratory
1-217-244-4392
Urbana, IL, USA

Tristan G. Rickett

rickett3@illinois.edu

University of Illinois at
Urbana-Champaign
Department of Civil and
Environmental
Engineering
Rail Transportation
Technology Center
(RailTEC)
1-217-244-6063
Urbana, IL, USA

Anirudh Vemula

vemula1@illinois.edu

University of Illinois at
Urbana-Champaign
Department of Civil and
Environmental Engineering
Rail Transportation
Technology Center
(RailTEC)
217-244-4392
Urbana, IL, USA

John M. Hart

jmh@vision.ai.uiuc.edu

University of Illinois at
Urbana-Champaign
Beckman Institute for
Advanced Science and
Technology
Computer Vision and
Robotics Laboratory
1-217-244-4174
Urbana, IL, USA
217-244-4392

J. Riley Edwards

jedward2@illinois.edu

University of Illinois at
Urbana-Champaign
Department of Civil and
Environmental
Engineering
Rail Transportation
Technology Center
(RailTEC)
1-217-244-7417
Urbana, IL, USA

Narendra Ahuja

n-ahuja@illinois.edu

University of Illinois at
Urbana-Champaign
Department of Electrical
and Computer
Engineering
Beckman Institute for
Advanced Science and
Technology
Computer Vision and
Robotics Laboratory
1-217-333-1837
Urbana, IL, USA

**Christopher P.L.
Barkan**

cbarkan@illinois.edu

University of Illinois at
Urbana-Champaign
Department of Civil and
Environmental Engineering
Rail Transportation
Technology Center
(RailTEC)
1-217-244-6338
Urbana, IL, USA

Abstract

Intermodal freight transportation is one of the largest sources of revenue for North American freight railroads and has experienced considerable growth over the past few decades. However, intermodal trains use rolling stock that generates significantly greater aerodynamic drag compared to other types of freight trains. The increased drag results in greater fuel consumption, which increases annual operating expenditures. There are opportunities to improve intermodal train aerodynamics by strategically placing the intermodal loads within the train's consist. A machine vision system is being developed to automatically monitor and analyze an intermodal train's aerodynamic efficiency based on the container/trailer loading pattern and the gap lengths between them. This system's main components are train detection sensors, a digital camera, video acquisition software, machine vision and analysis software, and a communication network. An automated system coordinates these components for the video capture of in-service trains. The machine vision algorithms separate the train from the background in the video and assemble a panoramic image of the entire train. Using this panorama, the containers, trailers, and gaps between the loads are identified and measured. Following the successful development of a prototype system at an intermodal terminal in Illinois, USA, a fully automated machine vision system is being developed along the BNSF Railway's intermodal corridor from Chicago to Los Angeles in the USA. The outputs of this system include load pattern monitoring, gap length information, and aerodynamic scoring, which are used to evaluate the loading efficiency of each train. In addition to the machine vision system, research is being conducted to determine how intermodal terminal managers can improve their decision making so that intermodal train loading can be more energy efficient.

1.0 Introduction

One of the largest sources of revenue for North American railroads is the transport of intermodal freight. Intermodal traffic is continuing to grow as the United States' economy continues to recover [1]. Economies of scale make rail transportation a cost-effective option for intermodal freight movement. In comparison to truck transport, railway intermodal transport is more fuel efficient due to the low-friction, steel-on-steel interface between the wheel and rail; the closely coupled railcars; and the rolling stock capable of transporting multiple trailers and/or containers in a single unit. To maximize the benefits of railway intermodal transport, railroads evaluate their terminals on how well they load intermodal trains. This promotes better utilization of intermodal railcar slots, maximizing the revenue from each intermodal train.

Despite its fuel efficiency, intermodal freight rail consumes more fuel than other freight types. In 2007, Class I railroads spent \$12.2 billion on fuel, representing 25.8% of their total operating cost [2]. The increased fuel consumption is partially due to the high aerodynamic drag of intermodal trains caused by large gaps between loads. Therefore, an evaluative system that measures the gaps between loads may be of relevance to railroads interested in improving the energy efficiency of their intermodal trains. This paper describes the development of a machine vision system that analyzes intermodal train loading and aerodynamics.

2.0 OVERVIEW OF INTERMODAL TRAIN LOADING METRICS

2.1 Slot Utilization

To understand how to improve intermodal train loading, it is important to first understand how intermodal train loading is evaluated. In North America, at least two loading metrics are used: slot utilization and train feet per unit. Slot utilization, the most common loading metric, is defined as the percentage of slots on a train that are filled with either trailers or containers. Slot utilization promotes the use of all slots for all rolling stock within the train, including double-stacked containers in well cars. For example, a five-unit articulated well car with a double stack in four wells and a single stack in the middle well has a slot utilization of 90% (Figure 1a). If a container were added to the top of the middle well, the slot utilization would be 100% (Figure 1b). The simplicity of calculation make the slot utilization metric a useful tool to determine intermodal train capacity.

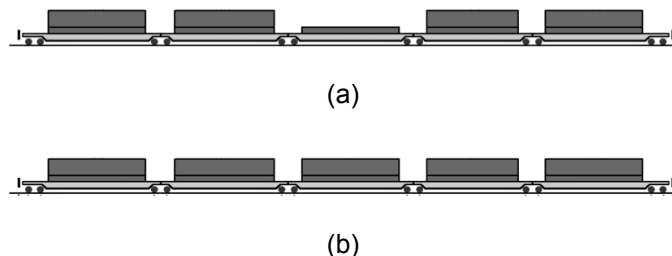


Figure 1: A five-unit well car with (a) 9 of the 10 slots filled and (b) 10 of 10 slots filled

2.2 Train Feet per Unit

One Class I railroad recently adopted a new loading metric called train feet per unit (TFPU). A train's TFPU is calculated by summing the out-to-out length of all the railcars in the train and dividing the sum by the number of loads on the train. Like slot utilization, TFPU can be measured as a percentage; the ideal TFPU of a train is divided by its actual TFPU. Table 1 shows the ideal TFPU values for various railcar and load combinations [3]. Referring back to Figure 1, if the railcar's outside length is assumed to be 260 feet (79.2 m) (5 cars with 48-foot (14.6 m) wells), then the Actual TFPU for (a) is $260/9 = 28.89$ ft/unit (8.8 m/unit), giving a TFPU utilization of $26.00/28.89 = 90\%$. For Figure 1b, the ideal and actual TFPU values are equal, so the TFPU utilization is 100%.

Table 1: Ideal TFPU values for various railcar and load combinations

Description	TFPU Value
Spine Cars	60 ft/unit
Single Stack Well Cars with Domestic Containers	70 ft/unit
Double Stack Well Cars with Domestic Containers	35 ft/unit
Single Stack Well Cars with International Containers	53 ft/unit
Double Stack Well Cars with International Containers	26.5 ft/unit

2.3 Slot Efficiency

A third loading metric that can be used to evaluate intermodal trains is slot efficiency [4]. Slot efficiency considers not only the length of wells or platforms but also the length of the units. Including the load lengths in the metric enables a more detailed comparison between the actual and ideal load configurations. Referring back to Figure 1, 40-foot (12.2 m) containers double-stacked in a 48-foot (14.6 m) slot well car would have a slot efficiency of 83%. Replacing the 40-foot (12.2m) containers with 48-foot (14.6 m) containers would make the slot efficiency 100%. Including slot and load lengths also makes slot efficiency an excellent tool to evaluate how well loads and platform/well sizes are matched, which can help in determining the energy efficiency of intermodal trains.

2.4 Load Gap Lengths

North American intermodal rolling stock consists of flat cars, spine cars, and well cars (Figure 2). These cars have a variety of designs and loading capabilities, which result in varying gap lengths between loads on adjacent railcars or platforms/wells. If gaps between loads exceed 6 feet (1.8 m) in length, the loads are aerodynamically separate and the aerodynamic drag increases significantly due to the change in the boundary layer [5]. In addition to equipment variety, intermodal freight trains are among the fastest trains operated by North American freight railroads. Intermodal trains are often operated at speeds of up to 70 miles-per-hour (mph) (112 km/h), to remain competitive with highway trucks that have traditionally offered more reliable and flexible service. The resulting high speeds and poor aerodynamics of intermodal trains result in high train resistance and fuel consumption.

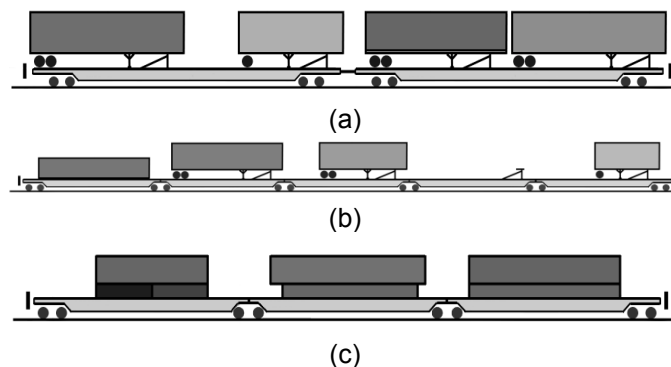


Figure 2: Typical North American intermodal rolling stock: (a) two-unit flat car with trailers (b) five-unit articulated spine car with a container trailers, and (c) three-unit articulated well car with containers

2.5 Train Resistance and Fuel Consumption

Train resistance is the summation of the frictional and other forces that a train must overcome in order to move [6]. The general equation for train resistance is $R = AW + BV + CV^2$, where A is the bearing resistance, B is the flange resistance, and C is the aerodynamic resistance [6]. The A term varies linearly with the weight (W) of the railcar or train, the B term varies linearly with train speed (V), and the C term varies exponentially with train speed. The exponential relationship between aerodynamic resistance and train speed means that aerodynamic resistance significantly impacts train resistance and, consequently, fuel consumption. To show the impact of aerodynamic resistance, Paul et al. [7] referenced the following equation used to estimate fuel consumption based on a train's weight, speed, and aerodynamic drag:

$$(1) \quad FC = K(0.0015W + 0.00256S_d V^2 + CW)$$

Where

FC = the fuel consumption in gal/mi

K = the fuel consumed per distance of traveled per unit of tractive resistance = 0.2038

W = the train's total weight (lb)

S_d = the consist drag area (ft²)

V = the train's speed (miles/hr)

C = Hill Factor = 0.0 for level routes and 0.0007 for hilly routes

A comparison of train drag areas by railcar type is shown here in Figure 3, where each train consists of 3 locomotives and 90 railcars.

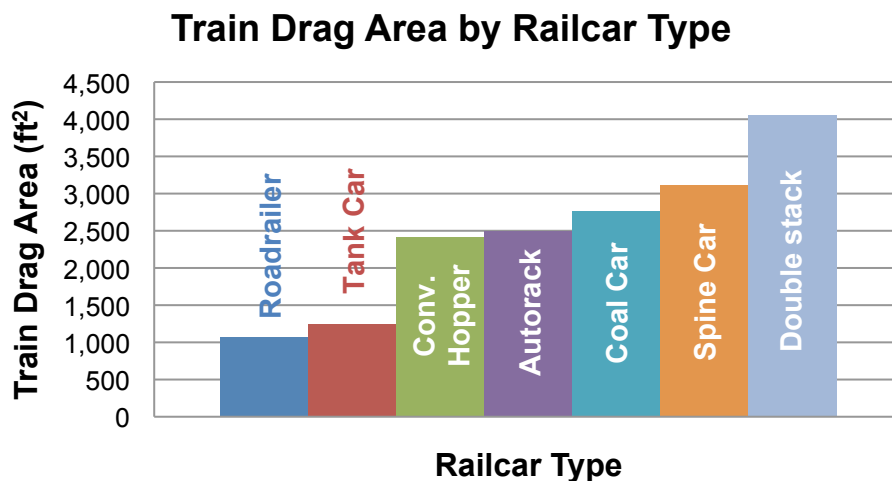


Figure 3: Comparison of railcar drag areas

Using the fuel consumption equation from Paul et al., a train traveling at 70 mph consisting of 3 locomotives with 53-foot, double-stack containers in thirty, 3-unit railcars traveling at 70 mph can have its fuel consumption reduced by 0.1 gallons per mile for each percent reduction in the train's drag area. Reducing aerodynamic drag over thousands of miles can result in a significant savings in operations costs.

Aerodynamic resistance can be reduced by several methods, including improved intermodal rolling stock design, aerodynamic reduction attachments [7], improved container/trailer design [7], reduced train speed, and improved terminal loading practices [4]. Redesigning railcars or containers/trailers requires a significant capital investment and is limited to designs compatible with existing container and trailers types. Improved loading practices can provide an economical alternative for reducing aerodynamic resistance.

2.6 Optimizing Intermodal Train Loading

Researchers at the University of Illinois at Urbana-Champaign (UIUC) investigated methods for optimizing intermodal loading to reduce gap lengths between containers/trailers. Lai and Barkan discussed how the potential savings of switching to slot efficiency can be as much as 1 gallon of fuel per mile (2.35 liters of fuel per kilometer), depending on the specific rolling stock and the loads available [4]. Subsequently, Lai, Barkan, and Onal developed an optimization model that minimized a train's gap lengths given specified loads [8]. Lai, Barkan, and Ouyang further expanded this optimization model to account for loading multiple trains simultaneously and for the uncertainty of incoming loads [9]. In addition to modeling, the BNSF Railway is funding a UIUC research project to develop a machine vision system that will be used as a diagnostic tool to evaluate current train loading practices and future loading improvements.

3.0 WAYSIDE VIDEO ACQUISITION OF INTERMODAL TRAIN LOADS

A primary goal of the machine vision system is to capture the current configuration of the loads on each intermodal train traveling along the BNSF Transcon. The system records a video of each train

that passes by the wayside installation. The stages of development involved in the construction of the wayside station are described below.

3.1 Mobile System Setup

The interdisciplinary team from UIUC visited various mainline locations to record videos of intermodal trains and experiment with various lenses, camera positions, and angles. Initially, a portable video acquisition system consisting of a laptop computer, a tripod, and a camera was used at single-track locations to ensure that no other trains would be visible in the video. The camera exposure was manually adjusted before the video was captured to compensate for the current environmental conditions. The images from these initial videos were processed to determine the best camera position and orientation for the development of the machine vision algorithms.

3.2 Semi-permanent Wayside Installation in Joliet, Illinois, USA

After experimenting at various wayside locations with the portable video acquisition equipment, the next step was to develop a wayside installation that could record intermodal traffic passing by on a daily basis. BNSF's Logistics Park, Chicago (LPC) was an ideal location for a test installation. Approximately eight to ten intermodal trains pass through LPC per day, and the intermodal terminal provided easy and safe access for developmental work.

To select a specific site for the wayside installation within the terminal, special attention was paid to the relationship between the site location and the track. The wayside installation needed to be alongside a single track to ensure that only one train could appear in the camera view at a time. Ideally, the camera view needed to face south to prevent direct sunlight from entering the camera lens during sunrise or sunset. A location perpendicular to tangent track on the northern section of the loop track provided the best view of the train. The camera was mounted on an adjustable 6-foot (1.8 m) tower and was protected inside an enclosure. Experiments were conducted to develop an auto-exposure routine that would allow the camera to adjust to the current environmental conditions. A target was also installed to adjust the exposure of the videos before the train reached the camera.

A simple, automated acquisition routine for video capture was developed to detect an approaching train. The routine allowed the camera time to adjust the exposure and start recording the video prior to the arrival of the train. Two wheel detectors were installed at each end of the site, approximately 300ft (91.4 meters) from the camera. When the first wheel of the locomotive trips the detector, a signal is sent to the on-site computer. A data acquisition board in the computer reads this signal, sets the camera exposure, and begins the video recording. The computer and other hardware are stored inside a small aluminum enclosure to shield them from the environment. The LPC installation was also equipped with an R&D automatic equipment identification (AEI) reader provided by the construction contractor, which converts the raw data into a useable format. In addition, a communication system was installed that enabled the train videos and the AEI data to be transferred over the internet to the Computer Vision and Robotics Lab at UIUC.

The LPC installation has been valuable in proving the feasibility of the wayside installation concept and in testing the load identification algorithms. However, the majority of LPC trains are container trains, which does not reflect the variety of intermodal rolling stock equipment and loading permutations in revenue service. After the success of the LPC installation, the development of a second installation was requested to analyze trains in revenue service at a mainline location.

3.3 Mainline Installation at Sibley, Missouri, USA

Currently, BNSF and UIUC are developing a fully automated wayside system along BNSF's Southern Transcon near Sibley, Missouri. This is an ideal location for a revenue service installation because it has about 40 to 50 intermodal trains a day over a single-track section of the Transcon. Many of the intermodal trains travel to/from Chicago and Los Angeles and loading improvements on these trains would result in substantial fuel savings along this over 2,000-mile (3218 km) corridor. Figure 4 provides a plan view diagram of the Sibley installation that includes all detectors with their distances measured relative to the camera installation.

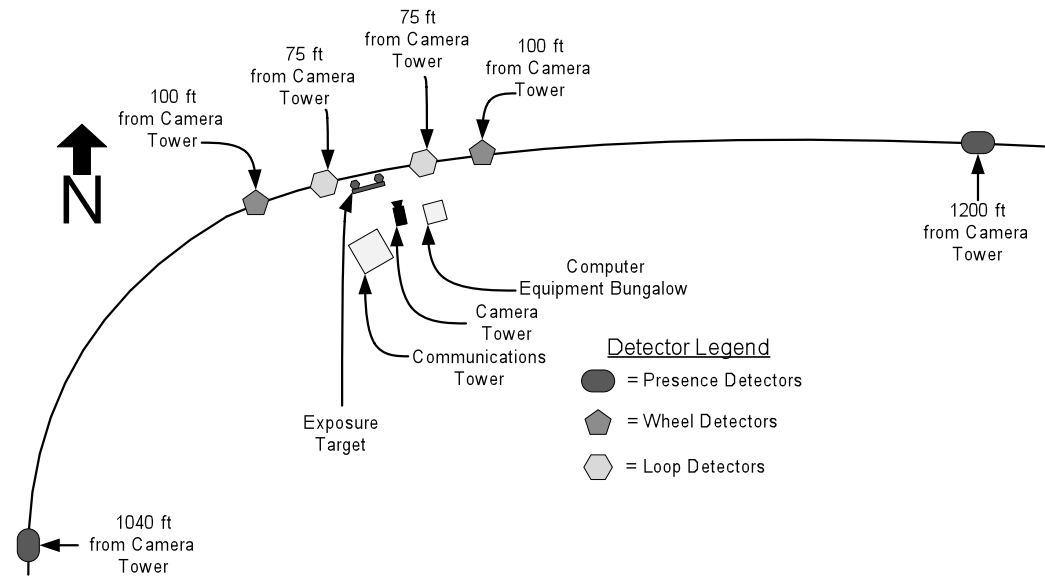


Figure 4: Plan view of Sibley installation

At this installation, a more sophisticated video acquisition system has been developed, which is similar to LPC in that it has a camera tower with an enclosure to house the camera, a bungalow to house the computers, detector electronics, and a target near the track for adjusting the camera exposure as shown in Figure 5. Additionally, there are three types of train detectors, each with different capabilities and functions. The outermost detectors are called presence detectors and are located 1,000 to 1,200 feet (304 to 366 meters) from either side of the camera location. These detectors use microwave technology to detect trains and send wireless signals to inform the detector electronics inside the bungalow that a train is approaching. These detectors provide enough set-up time for the video acquisition system. The wireless detectors also help in reducing the installation costs for trenching cables along the BNSF right-of-way. Resonant-type wheel detectors are also located on either side of the camera but are closer than the presence detectors (at 75 feet [22.8 meters]). They send a pulse to the computer when a locomotive or railcar wheel passes over the detector, which triggers the start of video acquisition. These detectors minimize the effects of slow train speeds on the length of the video by waiting until the train is very close to the camera before starting the acquisition. The third kind of detectors are inductive loop detectors, which are located in front of the camera. The loop detectors transmit a continuous signal if there is a train above them. The need for the loop detectors is to verify whether a train has stopped within the installation, since the other detectors are dependent on the motion of the train.

Although, due to the remote location of the installation, the communications system currently has a slower wireless connection from a card provided by a cellular phone service, yet the communication speed is fast enough to enable a remote connection for various critical tasks ranging from software testing to maintenance of machine vision software. Therefore, transferring of videos for prototyping and testing of the machine vision system at UIUC is currently done by first moving it to external hard-drives at the site and then shipping them to UIUC. In 2010, an AEI reader with redundant transponder detection capabilities was installed and integrated with the wayside automation subsystem at the site.



Figure 5: Southern view of the Sibley machine vision installation, showing from left to right, the AEI reader, equipment bungalow, camera, communication tower and exposure target

A custom, machine-vision automation system has been designed to integrate various sub-systems, such as, train detection, camera triggering, video acquisition and machine vision based analysis of the video. Specifically, the main objectives for the automation system are the following:

1. Detect the status of incoming trains
2. Execute the different sub-systems as the train approaches and passes the installation
3. Distribute the resulting data files between the different sub-systems for further processing
4. Control the sub-systems to adapt to changing environmental conditions

When completed, the automation will execute the software for analyzing and scoring the trains on-site and transfer results information to BNSF directly. The next section describes the design of the machine vision based intermodal train analysis system including various techniques which have been applied to extract relevant information (e.g. gap lengths) using only the captured video.

4.0 IDENTIFICATION AND MEASUREMENT OF LOADS USING MACHINE VISION ALGORITHMS

This section describes the design and implementation of the Train Monitoring System (TMS) that uses computer vision and image processing algorithms to process an intermodal train video and obtain the lengths of gaps between consecutive loads on the train. TMS is divided into various modules as described by the block diagram in Figure 6.

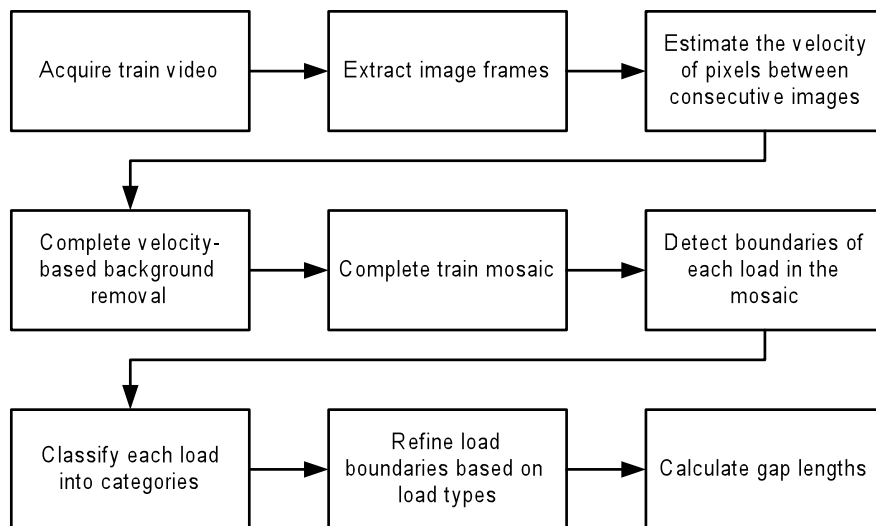


Figure 6: Flow of Train Monitoring System starting with acquisition and ending with calculation of the gap lengths between loads

The first stage consists of acquiring the video using a PGR Flycap camera whenever it is triggered by the various detectors (described in Section 3.3). Each video is made up of image frames of size 640 x 480, which have been captured at 30 frames per second (fps). The beginning of the video contains only the background, made up of trees, clouds and other scenery. Then, after a short period of time, the intermodal train enters the field of view of the camera and thereafter the video consists of the intermodal train as it passes in front of the camera. The camera continues recording until the train clears the site. Thus, the train video is composed of two kinds of image frames:

- Type I: Background is visible without any train image (beginning and the end of the video)
- Type II: Parts of the train along with background visible through the gaps of and above the train (remaining video)

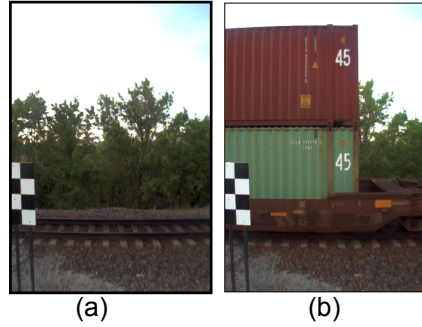


Figure 7: (a) Type I (b) Type II image frames

As the train is visible in Type II image frames, the next goal is to extract regions belonging to train in these images. This has been described in the next section.

4.1 Computation of train velocity

An image frame is made up of small rectangular blocks called as pixels, each having an associated value for the amount of red, blue and green color in them based on the color of the scene point it images. In TMS, the color values are converted to one single value by averaging the three color values. This generates an image where all of the pixels are a shade or intensity level of gray. Now, the task is to identify the train in each image frame of the video. This is done by first computing the amount by which all pixels in an image have moved between consecutive image frames. The movement of pixels can be measured accurately because the gray level intensity of any object in the image remains almost the same between consecutive image frames. By finding the location of similar pixels in consecutive image frames reliably, pixel movement can be defined by the difference of those locations. This is also known as optical flow problem in the field of computer vision [12]. In this paper, we will refer to it as pixel motion or pixel velocity. Also, from the knowledge that trains move fast compared to other background objects like trees and clouds in the image, it can be inferred that high velocity pixels must belong to the train. By finding regions with high pixel velocities, we can identify regions in the image which belong to the train and background respectively. In the next paragraph, we describe a technique which is robust to image noise and low texture regions for computing pixel velocities of all pixels in a given image frame.

For our technique, it is required to keep an updated estimate of the background after processing each image frame. It is assumed that the first image frame in the video is always the background. Thus, this frame becomes the current estimate of the background when we start processing any intermodal video (we start from the second image frame). After computation of train region (i.e. the background region also) in the second image frame, the background estimate is updated. This is repeated as we sequentially process all image frames in the video. Such updates give us the latest estimate of the background and are useful in computation of pixel velocities for later image frames in the video.

Let the current image frame requiring pixel velocity computation be denoted as I_c (c for current). Let I_p (p for previous) and I_n (n for next) denote image frames which were captured previous to and next to I_c respectively. Also, let I_{bg} (bg for background) denote the current estimate of the background as described in the previous paragraph. It is known that a rail car will always be visible in an intermodal train video, with or without a load on it, its location in consecutive image frames can be used to obtain an initial estimate of train's velocity. This is accomplished by correlating the common parts of railcar visible in I_c and I_n (or I_c and I_p) and obtaining an initial velocity estimate v . It can be noted that this velocity indicates the motion of the complete train in that image frame as compared to being a single pixel velocity. The individual pixel velocities are calculated as follows.

Once the initial velocity v is obtained, the next step is to find regions in the current image I_c which are moving with that velocity. These regions are found by taking a window of size S_z (21×41 pixels) in image frame I_c at all locations (x,y) and correlating it with a window of same size in image frame I_p at location $(x-v,y)$ and in image frame I_n at location $(x+v,y)$. The correlation metric used is normalized cross correlation (NCC) [11]. The above computation assumes that the train only moves horizontally, which is reasonable as it is observed that there is only negligible vertical motion of the train between consecutive image frames.

NCC requires preprocessing of each window S_z as follows. The mean pixel intensity of the window is subtracted from each pixel value in the window to reduce the effect of lighting changes. Then, all the pixel values in this window are normalized such that their sum of squares is equal to 1. At each window patch located at (x,y) in I_c , two NCC costs are calculated, NCC_p and NCC_n , corresponding to correlations with previous image frame (I_p) and next image frame (I_n) respectively. In addition to these two correlations, the window located at (x,y) in the current image frame I_c is correlated with the window located at (x,y) in I_{bg} , which is the image of the current background estimate and is being maintained at each iteration of our algorithm. This correlation value, stored as NCC_{bg} will be high if S_z belonged to a region in the background in I_c . Finally, all the correlation values are combined together to obtain a cost for the pixel centered in the window S_z to belong to foreground. This value is called as FG_{Cost} and is calculated as follows:

$$FG_{Cost} = \frac{(NCC_p + NCC_n - 2 \times NCC_{bg})}{4}$$

Figure 8 explains the above technique. The denominator in the equation normalizes the FG_{Cost} between -1 and 1. As can be seen from the cost function, if the window S_z belonged to the foreground, then NCC_p and NCC_n will be high (close to 1) and NCC_{bg} will be low (close to -1). This will make the FG_{Cost} close to 1. Alternatively, if the window belonged to background then each one of NCC_p and NCC_n will be close to -1 if the background is textured (e.g. sky with clouds) or close to 1 if the background is texture-less (e.g. clear sky). However, in this case the NCC_{bg} cost will always be close to 1 because the current window will correlate with high value with background. Thus the FG_{Cost} will lie somewhere between -1 and 0.

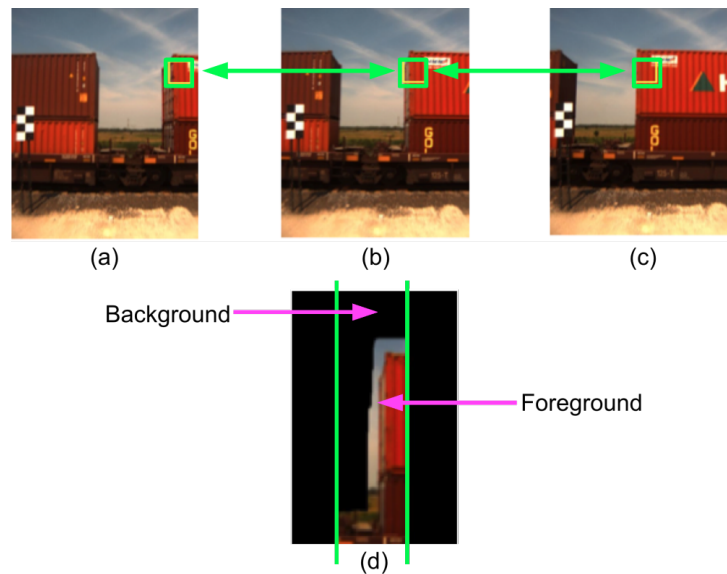


Figure 8: Normalized correlation calculated between image frames (a) I_p at $(x-v, y)$ (b) I_c at (x, y) (c) I_n at $(x+v, y)$ and (d) the background removed from image I_c

4.2 Background Removal

Based on the computation above, the foreground cost will be close to a value of 1 for pixels belonging to the train and to a value less than or equal to 0 for other background pixels. Therefore, the system then assigns the label of foreground to all pixels with a foreground cost greater than some value T and assigns the label of background to all other pixels. The experiments suggest that setting $T = 0.2$ (FG_{Cost} lies between -1 and 1) yields the largest number of successful results.

4.3 Mosaic Generation and Load Detection/Classification

Once the velocity of the train is obtained, strips having a width equal to the velocity v are taken from I_c and are used to comprise the panoramic image. This process is continued for all of the image frames in the video, creating a seamless panorama of the entire train, known as a mosaic. By using the particular velocity v calculated for an image frame as the width of the strip extracted from that image frame, it is made sure that the panorama doesn't contain duplicated or missing parts of the train. As v might change between consecutive image frames, such a mosaic building technique makes sure that

the algorithm is adaptive to changing train speeds while it is passing in-front of the camera and being captured. Figure 9 shows a panorama of the complete train with its background removed.

Once the mosaic is generated, the outer boundaries of all the loads on the train can be detected. To illustrate the meaning of the term outer boundaries, consider a double-stacked load with a large container on top of a small container. For this load, the outer boundary would be the edge of the large container. Since the edge of the smaller container is not detected as part of the outer boundaries, additional algorithms are needed to detect the other edges. For the loads to be classified into categories TMS must detect all load edges within the train video.



Figure 9: Two horizontal strips showing a portion of an intermodal freight train panorama

The first step in load classification is to identify each load as a single or double stack based on its height. TMS uses data on the height of single stacks and known camera parameters to calculate the threshold height. If the top of a load lies below the threshold height, it is labeled as a single stack. A sample detected single stack is shown in Figure 10.

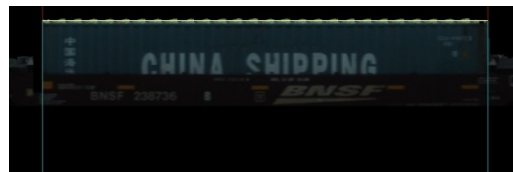


Figure 10: Single Stack detected

If the top of a load rises above the threshold height, it must be either a trailer or a double stack. The trailers are characterized by having some amount of background visible near their bottom. Thus, TMS looks for a block of pixels near the bottom of a load whose intensity is close to that of the background. When such a block of pixels is detected, TMS labels the load as a trailer. Figure 11 shows a trailer correctly detected using this technique.



Figure 11: Trailer detected

When TMS does not detect background near the bottom, the load is classified as a double stack. However, a double stack load can have three different configurations: a long container on a short container, a short container on a long container, or two containers of the same length. Since these different configurations have different edge boundaries, gap lengths involving double-stacked loads will vary. Therefore, it is necessary to detect the type of double stack in order to obtain accurate gap information. To detect the type of double stack, a window of an arbitrary size is taken from the center of the load. The intensity values in this window are projected horizontally by summing them to form a vector of intensity values. The location of the minimum intensity value in this vector corresponds to the location of the *middle line* of the double stack, which is defined as the boundary line between the upper and the lower stack (Figure 12).

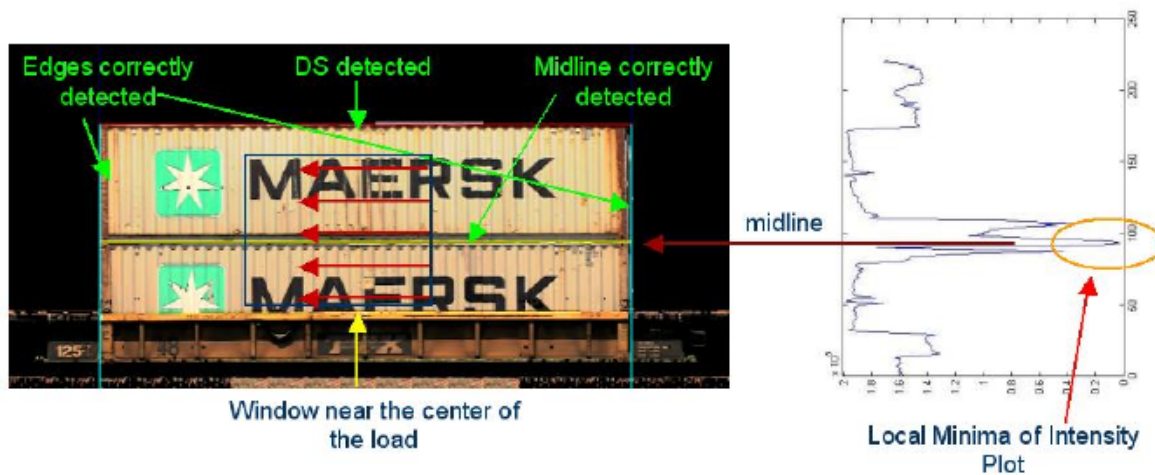


Figure 12: Determining the middle line of a double stack

To determine the relative size of the lower and upper containers, two windows are chosen above and below the middle line near the left boundary. TMS performs a simple background subtraction in the image frame from which the windows are taken and obtains a coarse estimate of the foreground. TMS then projects the extracted foreground image vertically in the windows and finds the location of steep change. The steep change corresponds to the edge of the short container. This process is repeated for the right boundary of the double stack. The sizes of the containers are then calculated using a pixel-to-foot conversion determined by the camera and lens parameters and the location of the camera relative to the track. The results are shown in Figure 13(a-b).

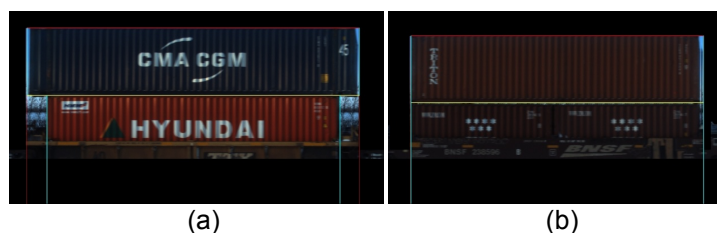


Figure 13: (a) Double stack with a larger container on top (b) Double stack with one load having same sized containers

Once the container/trailer sizes are determined, the gap lengths between loads are calculated by measuring the distance between the boundaries of consecutive loads. The train's loading can then be evaluated by the Train Scoring System.

5.0 ANALYSIS OF INTERMODAL TRAIN LOADING AND AERODYNAMICS

The Train Scoring System (TSS) evaluates intermodal train loading efficiency and provides a train-specific aerodynamic coefficient using the gap-length information obtained from the TMS. In order to attain these results, the TSS requires the following input data: a portion of the Universal Machine Language Equipment Register (UMLER) database pertaining to intermodal rolling stock, AEI data, and TMS result data. Figure 14 describes the flow of data through the major subroutines in the train scoring system.

5.1 Train Scoring System

The UMLER database contains design and loading information of all railcars in unrestricted interchange within North America. We use a subset of the UMLER (mini-UMLER) database pertaining to intermodal rolling stock, which includes the car identification number, outside length, loading attributes, and other geometric and operational parameters. The loading attributes also describe whether the railcar has one, three, or five units (the three or five-unit cars are articulated cars that are connected by drawbars). Additionally, data fields describe whether the railcar can transport containers and/or trailers and what load sizes can be accommodated. Using this information from UMLER, TSS determines the ideal loading configurations for each railcar in the train. The second input is the AEI data that includes the order of the railcars and a timestamp for each axle. The AEI data is obtained from an AEI reader at the site which identifies each railcar and locomotive

name and number in the passing train. The axle timestamps, which are collected from the AEI reader using a wheel detector, help match the loads identified in TMS with the correct railcar platform or well identified from the AEI tag data. The railcar identification and number is then used to query mini-UMLER to determine the railcar's loading capabilities.

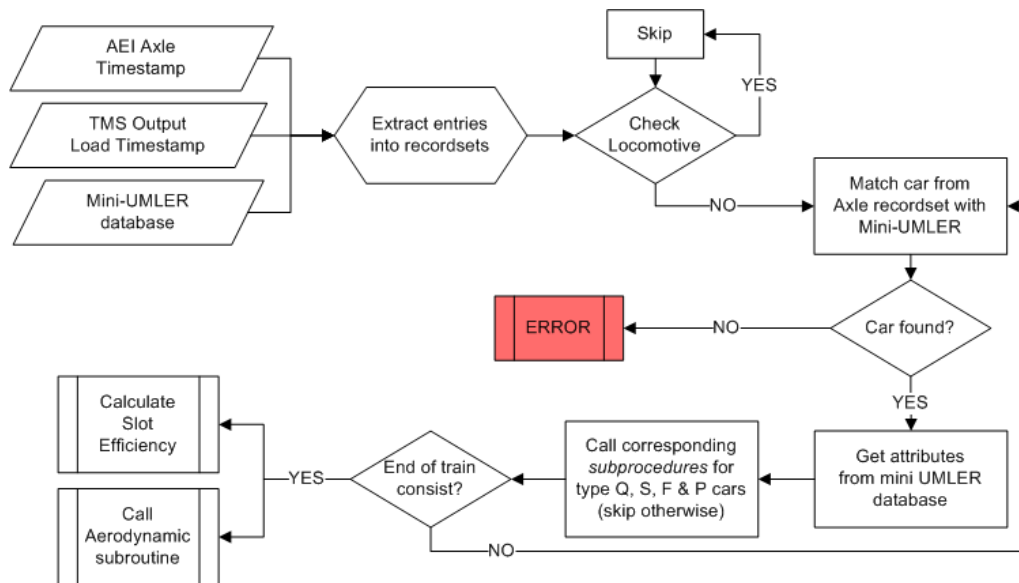


Figure 14: Flow Diagram of TSS describing the relationship between input data, major subroutines and the outputs

To align these loads on corresponding cars, TSS first extracts the number of wells/platforms for each car in the train using AEI data and mini-UMLER. It then compares the timestamps of axles on either side of a well/platform with the start and end times of the load, ignoring the cars which have been skipped earlier (with invalid number of wells/platforms; or not found in mini-UMLER). If the start time of the load is greater than the starting axle timestamp, and the end time is less than the ending axle timestamp of a well, then the load is said to have been matched. For each of these matched loads, it calculates corresponding gap lengths and final train score by comparing with the optimal loading configuration.

5.2 TSS Results Summary

The final result of the TSS is a text file that contains the slot efficiency for each slot in the train (for well cars, it includes both the bottom and top containers) and a value for the average slot efficiency for the entire train. Also, the aerodynamic coefficient is calculated so that the train's fuel consumption can be computed by the Association of American Railroad's (AAR's) Train Energy Model (TEM). This software uses aerodynamics, weight, train handling, and the route characteristics to obtain a very accurate estimate of train fuel consumption. From the preliminary results of 30 trains, the average slot efficiency was 83% and the average aerodynamic coefficient was 5.98 lb/mph². This preliminary analysis of the TSS results show that the trains are well loaded and aerodynamic but there is indeed opportunity to further improve train aerodynamics. In the future, TSS output data will be transferred to BNSF to evaluate the loading performance of a particular terminal, train, and/or terminal manager.

6.0 FUTURE WORK

Automation software for implementing the remaining machine vision sub-systems is being refined, which will allow for automatic TMS and TSS processing at the Sibley installation. However, it must be ensured that the increased processing time does not interfere with the video acquisition. In addition, improvements are being made to the TMS background removal process to reduce errors in gap length determination. A detailed analysis of the TMS load edge and gap measurement accuracy is also underway. TSS results are being prepared that will evaluate the present loading performance of intermodal trains traveling along the Transcon and identify the common loading configurations that contribute to reduced aerodynamic efficiency.

The next phase of the study will be to investigate the potential consequences of altering loading practices, which may include lost efficiency and/or productivity at the terminal. This study will compare the time needed for a well-loaded and a poorly-loaded train to complete loading. Using data from terminals, the costs of improved loading practices will be compared to the benefits of improved energy efficiency. If improved loading practices prove to be beneficial, this machine vision system can then serve as a valuable measurement tool to track improvements and consequent fuel savings.

ACKNOWLEDGEMENTS

The authors would like to thank the BNSF Railway and BNSF's Technical Research and Development (TR&D) department for funding this research project. Specifically, the authors would like to thank Mark Stehly, Larry Milhon, Paul Gabler, and Josh McBain for their expertise and guidance throughout this project. Also, we would like to thank Leonard Nettles and Kevin Clarke from LJN and Associates for their assistance with the construction of the Sibley, MO installation. J. Riley Edwards has been supported in part by grants to the UIUC Railroad Engineering Program from CN, CSX, Hanson Professional Services, Norfolk Southern, and the George Krambles Transportation Scholarship Fund.

REFERENCES

- [1] Association of American Railroads. Class I Railroad Statistics. Washington, D.C., May 24, 2010.
- [2] Association of American Railroads. Railroad Facts 2009. Washington, D.C., 2009.
- [3] White, Lex. Personal Communication. CSX Intermodal.
- [4] Lai, Y.C., and C.P.L. Barkan. Options for Improving the Energy Efficiency of Intermodal Freight Trains. *Transportation Research Record*, No. 1916, Transportation Research Board of the National Academies, Washington, D.C., 2005, pp. 47-55.
- [5] Engdahl, R., R.L. Gielow, and J.C. Paul. Train Resistance—Aero- dynamics Volume I, Intermodal Car Application. *Proc., Railroad Energy Technology Conference II*, Atlanta, Ga., Association of American Railroads, 1986, pp. 225-242.
- [6] Hay, W.W. *Railroad Engineering*, 2nd ed. John Wiley and Sons, New York, 1982.
- [7] Paul, J.C., R.W. Johnson, R.G. Yates. Application of CFD to Rail Car and Locomotive Aerodynamics. *The Aerodynamics of Heavy Vehicles II: Trucks, Buses, and Trains*, pp. 259-297, 2009.
- [8] Lai, Y.C., C.P.L. Barkan, and H. Önal. Optimizing the energy efficiency of intermodal freight trains. *Transportation Research, Part E 44*, 2007, pp. 820-834.
- [9] Lai, Y.C., C.P.L. Barkan, and Y. Ouyang. A Rolling Horizon Model to Optimize the Aerodynamic Efficiency of Intermodal Freight Trains with Uncertainty. *Transportation Research, Part E 44*, 2007, pp. 820-834.
- [10] Association of American Railroads, Loading Capabilities Guide, Washington D.C., May 19, 2009.
- [11] Lewis, J. P. Fast Normalized Cross-Correlation, 1995. <http://www.idiom.com/~zilla/Work/nvisionInterface/nip.html>. Accessed August 1, 2010.
- [12] B.K.P. Horn and B.G. Schunck, Determining optical flow. *Artificial Intelligence*, vol 17, pp 185-203, 1981.